INSTITUTE OF PHYSICS PUBLISHING JOURNAL OF PHYSICS D: APPLIED PHYSICS

J. Phys. D: Appl. Phys. **38** (2005) 1402–1409 doi:10.1088/0022-3727/38/9/012

Improvements to a scale-dependent model for contact and friction

George G Adams and Sinan Müftü

Department of Mechanical and Industrial Engineering, Northeastern University, Boston, MA 02115, USA

E-mail: adams@neu.edu and smuftu@coe.neu.edu

Received 29 September 2004, in final form 22 February 2005
Published 22 April 2005
Online at stacks.iop.org/JPhysD/38/1402

Abstract

In this investigation three effects are included in a recently developed scale-dependent multi-asperity model of elastic contact and friction. First, a Weibull distribution of asperity heights is used, which allows the skew and kurtosis to be varied, but not independently of each other. Second, the effect of non-constant radii of curvature of the asperity summits, with the curvature varying with asperity height, is examined. Finally, the influence of noncontacting asperities on the normal force and hence on contact and friction is included. It is noted that the contact and friction model used (Adams *et al* 2003 *ASME J. Tribol.* **125** 700–8) includes the effects of adhesion and scale-dependent friction. It is demonstrated that positive/negative skew decreases/increases both the friction coefficient and its dependence on the normal load. The results also indicate that for radii of curvature that increase/decrease with height, the friction coefficient increases/decreases as does its dependence on load.

1. Introduction

Contact and friction affect the operation of many machines and tools that we use every day, as well as some of the most basic activities in nature. Examples range from belt drives, brakes, tyres and clutches in automobiles and in other machines; gears, bearings and seals in a variety of mechanical systems; electrical contacts in motors; slider–disk interactions in a computer disk drive; various MEMS devices; robotic manipulator joints; the motion of a human knee-joint (natural or artificial) and walking/running.

The frictional force F is the tangential force resisting the relative motion of two surfaces which are pressed against each other with a normal force P. Amontons, in 1699, and Coulomb in 1785, developed our phenomenological understanding of dry friction between two contacting bodies. Amontons–Coulomb friction states that the ratio of the friction force (during sliding) to the normal force is a constant called the coefficient of kinetic friction. Similarly, the coefficient of static friction is the ratio of the maximum frictional force F that the surfaces can sustain, without relative motion, to the normal force. These friction laws can be summarized by defining the coefficient of friction μ as

$$\mu = \frac{F}{P}, \tag{1}$$

without distinguishing between static and low-speed sliding friction. Although equation (1) provides an extraordinarily simple *phenomenological* friction law, the *nature* of the frictional force is not well-understood.

Tabor [2] reviewed the state of understanding of frictional phenomenon as it existed two decades ago. Friction was originally thought to be due to the resistance of asperities on one surface riding over the asperities of the mating surface. The main criticism of this *roughness theory of friction* is that it is a conservative process whereas friction is known to be dissipative. Nonetheless, the terminology of 'smooth' and 'rough' to represent frictionless and frictional contact, respectively, still persists in, for example, many elementary mechanics textbooks.

The *adhesion theory of friction* relates roughness to friction in a different manner [2]. Because real surfaces always possess some degree of roughness (figure 1), the contact between two bodies occurs at or near the peaks of these contacting asperities. Thus, the real area of contact will generally be much less than the apparent contact area, and the average normal stress in the real contact area can easily reach the hardness of the softer material. If each asperity contact is viewed as a plastic indentation, then the normal contact stress is constant, and the real area of contact is proportional to the normal force. Thus, the adhesion theory of friction,

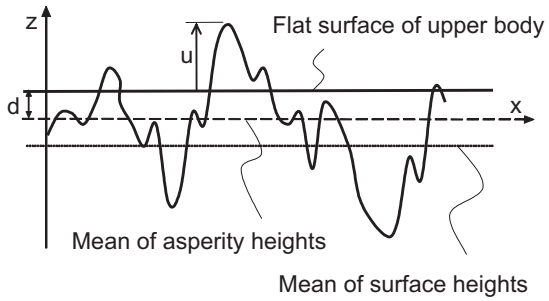

Figure 1. Contact of a rough surface (lower body) with a flat surface (upper body).

which gives a frictional force proportional to the real contact area, also gives the proportionality between the frictional force and the normal load required for Amontons–Coulomb friction, i.e. equation (1). However, even in the absence of plastic deformation, the real area of contact is nearly proportional to the normal load if the asperities have a statistical distribution of heights [3] and also leads to equation (1).

Thus, *contact modelling* is an essential part of any friction model. It consists of two related steps. First, the equations representing the contact of a single pair of asperities are determined. In general, this procedure includes elastic, elastic–plastic, or completely plastic deformation. For nanometre scale contacts, the effect of adhesion on the contact area is also included. Second, the cumulative effect of individual asperity contacts is determined. Such contact models are uncoupled and represent surface roughness as a set of asperities, often with statistically distributed parameters. The effect of each individual asperity contact is local and considered separately from the other asperities; the cumulative effect is the sum of the actions of individual asperities (e.g. the well-known Greenwood–Williamson model [3]).

In multi-asperity models, such as [3], the radii of curvature of all asperities are assumed to be equal. However, the curvature is likely to be height dependent due to, for example, polishing operations in which higher asperities are polished to a greater extent and, therefore, have larger radii of curvature than do the shorter asperities. On the other hand, from the point-of-view of a random surface profile, Whitehouse and Archard [4] found that higher asperities have smaller curvatures. This result is a consequence of the assumed randomness of a surface in which the neighbouring points about a *high* peak are more likely to have a height that deviates from the peak height by a greater amount than would the points near a lower peak. Extending the work of [4], Onions and Archard [5] found that such a distribution of asperity curvatures increases the contact pressures making plastic deformation more likely to occur.

For sufficiently small size contacts, the adhesion force between the surfaces affects the contact conditions. Various adhesion models, typically between an elastic sphere and a flat surface, have been introduced. The model by Johnson, Kendall and Roberts (JKR) assumes that the attractive intermolecular surface forces cause elastic deformation beyond that predicted by the Hertz theory, thereby producing a subsequent increase of the contact area [6]. The model by Derjaguin, Muller and Toporov (DMT), on the other hand, accounts for the adhesive stress outside of the contact area, but assumes that the contact stress profile remains the same as in the Hertz theory [7]. Due to the assumptions involved, the JKR/DMT models are most suitable when the range of surface forces is small/large compared to the elastic deformations, as pointed out by Tabor [8]. Another model, introduced by Maugis [9], describes a continuous transition between the JKR and DMT models.

Contact and friction models that deal with adhesion in multi-asperity contacts have also been developed. In the first of a series of papers Chang, Etsion and Bogy (CEB) [10] developed an elastic–plastic multi-asperity contact model for normal loading based on volume conservation of a plastically deformed asperity control volume. In [11], the effect of adhesion was included by using the DMT model for contacting asperities and the Lennard–Jones potential between noncontacting asperities. Finally, a model for calculating the coefficient of friction was given in [12]. It assumed that once plastic yielding is initiated in a pair of contacting asperities, no further tangential force can be sustained. Fuller and Tabor [13] developed a theoretical model that used the JKR model of adhesion along with a Gaussian distribution of asperity heights.

Stanley, Etsion and Bogy (SEB) [14] developed a model for the adhesion of two rough surfaces, affected by sub-boundary layer lubrication, in an elastic–plastic multi-asperity contact. Polycarpou and Etsion [15] used the SEB model to predict the static friction coefficient. The tangential load was found using the same procedure as in the CEB model [12] for solid–solid contact. Kogut and Etsion developed multi-asperity contact [16] and friction models [17], which included the effects of plastic deformation. The maximum shear load that an asperity can sustain is limited by the combined normal and shear load, which causes the plastic deformation zone to reach the surface. Thus, the friction analysis [17] predicts higher friction than the related work in [12].

The previously cited works used a Gaussian distribution of asperity heights. The effect of asymmetry in the height distribution has been accounted for by a few authors. Kotwal and Bhushan [18] modelled this effect and found that there are load-dependent optimal values of skew and kurtosis, which minimize the real area of contact. McCool [19] extended the GW model by using a Weibull distribution of asperity heights and by including the effect of a surface coating. The multi-asperity elastic–plastic CEB models were generalized to include a Weibull distribution by Yu and Polycarpou for contact [20] and by Yu *et al* for friction [21]. Skew was found to greatly affect the relation between the force, contact area and the number of contacting asperities. Positive/negative skew decreases/increases the friction coefficient.

The scale dependence of the friction stress for *single* asperity contacts has recently been investigated by Hurtado and Kim (HK) [22, 23]. They presented a micromechanical dislocation model of frictional slip between two asperities for a wide range of contact radii. According to the HK model, if the contact radius 'a' is smaller than a critical value, the asperities slide past each other in a concurrent slip process where the adhesive forces are responsible for the shear stress; hence, the shear stress remains at a high constant value. On the other hand, if the contact radius is greater than that critical value, the shear stress decreases for increasing values of contact radius until it reaches a second constant, but lower value. The relationship between the non-dimensional friction stress ($\bar{\tau} = \tau/G^*$) and

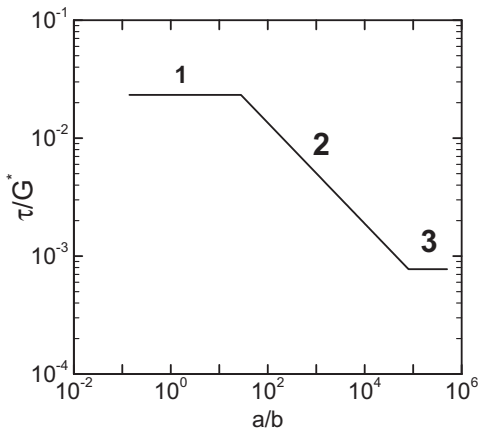

Figure 2. Relationship between friction stress and contact radius according to the HK model.

the non-dimensional contact radius ($\bar{a} = a/b$) is approximated in figure 2. The contact radius 'a' is normalized by the Burgers vector b and the friction stress (τ) is normalized by the effective shear modulus $G^* = 2G_1G_2/(G_1+G_2)$, where G_1 and G_2 are the shear moduli of the contacting bodies. It is noted that the dislocation motion is confined to the interface—the material behaviour remains elastic.

Adams, Müftü and Mohd Azhar (AMM) [1] developed a multi-asperity model for contact and friction by incorporating the adhesion contact model of Maugis and the scale-dependent HK friction model into a statistical model with a Gaussian distribution of asperity peaks. The relationship between the frictional force and the normal load between two rough surfaces during a slip process was determined. *Three key dimensionless parameters* were identified that influence friction and represent the surface roughness, the friction regime of the contacts, and the surface energy of adhesion. The friction coefficient increased as the load decreased. Experiments for multi-asperity contacts in the low and high normal load regimes have shown that *the friction coefficient depends on the magnitude of the normal force*. In particular, μ increases with decreasing normal load [24–26] which is qualitatively consistent with [1, 17].

In this paper, three effects are included in the AMM scale-dependent contact and friction model [1]. A Weibull distribution is used, which allows the skew and kurtosis of the asperity height distribution to be varied, but not independently of each other [27]. The effect of non-constant radii of curvature of the asperity summits, with the curvature varying with asperity height, is examined [28]. Finally, the influence of noncontacting asperities on the normal force and hence on contact and friction is included.

2. Multi-asperity contact and friction model

2.1. Asperity contact model

The scale-dependent multi-asperity contact and friction model developed by Adams *et al* [1] will be extended to include asymmetric asperity height distributions. For two real surfaces separated by a distance d (defined from the mean of asperity heights) the number of contacting asperities n is

$$n = N \int_{\bar{d}}^{\infty} \bar{\phi}(\bar{z})\, \mathrm{d}\bar{z}, \tag{2}$$

where N is the total number of asperities, σ the standard deviation of asperity peak heights, $\bar{z} = z/\sigma$ is the dimensionless height coordinate measured from the mean of asperity heights, $\bar{\phi}(\bar{z})$ is the probability density of asperity peaks and $\bar{d} = d/\sigma$ is the non-dimensional separation between the two surfaces (figure 1).

The height-dependent asperity radius of curvature is assumed to be of the form

$$R' = Rg(\bar{z}), \qquad g(\bar{z}) = 1 + \varepsilon \tanh(\rho\bar{z}), \tag{3}$$

where R is the average radius of curvature. The choice of the function $g(\bar{z})$ is somewhat arbitrarily chosen so that the asperity radius of curvature varies smoothly between $R(1-\varepsilon)$ and $R(1+\varepsilon)$. For positive ε, higher asperities have larger radii whereas for negative ε the higher asperities have smaller radii. For large ρ, the variation in radius with $\bar{z}$ occurs most abruptly in a small region surrounding the average asperity height, whereas for small ρ the variation is more gradual.

The relation between the normal load P and deformation $u = z - d$ of two contacting spherical asperities with adhesion is given by the Maugis model [9]. In that model, a uniform tensile stress σ_0 exists between the contacting asperities in an annular region just outside the contact zone, $a \leqslant r \leqslant c$, where c is the radial extent of the adhesion zone. The separation between the two surfaces at $r = c$ is taken to be equal to the prescribed maximum adhesion distance h. Thus, the work of adhesion is given by $w = \sigma_0 h$. Non-dimensional relations among the asperity contact radius ($\bar{a} = a/b$), the asperity contact force ($\bar{P} = P/Gb^2$) and the asperity deformation ($\bar{u} = u/\sigma$) are obtained based on [9]. Those relations are written in the form

$$\frac{\alpha b}{\pi\beta h g(\bar{z})}[\sqrt{m^2-1} + (m^2-2)\tan^{-1}\sqrt{m^2-1}]\bar{a}^2 + \frac{4\gamma b^2}{\pi h^2}[(m^2-1)\tan^{-1}\sqrt{m^2-1} - m + 1]\bar{a} - 1 = 0, \tag{4}$$

$$\bar{P} = \frac{8\alpha}{3\beta(1-\nu)g(\bar{z})}\bar{a}^3 - \frac{4\gamma b}{h(1-\nu)}[\sqrt{m^2-1} + m^2\tan^{-1}\sqrt{m^2-1}]\bar{a}^2, \tag{5}$$

$$\bar{u} = \bar{z} - \bar{d} = \frac{1}{\beta^2 g(\bar{z})}\bar{a}^2 - \frac{2\gamma b}{\alpha\beta h}\sqrt{m^2-1}\,\bar{a}, \tag{6}$$

where the non-dimensional adhesion radius (m) and the non-dimensional Maugis adhesion parameter (λ) are given by

$$m = \frac{c}{a}, \qquad \lambda = \left(\frac{b}{h}\right)\left(\frac{9\beta\gamma^2}{2\pi\alpha}\right)^{1/3} \tag{7}$$

and typically $b/h = 1$ is used.

In equations (4)–(6) there are three key parameters α, β and γ, which are defined as

$$\alpha = \left(\frac{\sigma}{R}\right)^{1/2}, \qquad \beta = \frac{(R\sigma)^{1/2}}{b}, \qquad \gamma = \frac{w}{E^* b}. \tag{8}$$

A physical interpretation of the parameters α and β is provided by noting that in a simple vertical scaling of the surface by a factor k, the standard deviation of asperity heights σ is scaled by k but the asperity radius of curvature R is scaled by $1/k$. Thus, α is scaled by k, but β remains constant. Hence, α is a representation of the surface roughness, and is referred to as the *surface roughness parameter*. The parameter β describes the ratio of the contact radius (due to an asperity penetration equal to σ) to the Burgers vector length. Thus, small β are expected to be indicative of nano-scale asperity contacts and progressively larger values of β correspond to transition and larger values of the contact radius (figure 2). Therefore, β is referred to as the *friction regime parameter*. The *surface energy parameter* γ represents the ratio of the adhesive stress to the product of the composite Young's modulus and the Burgers vector.

It is further noted that for the case considered here, in which one of the surfaces is assumed to be rigid and flat, $G^* = 2G$ and the composite Young's modulus is given by $E^* = E/(1-\nu^2)$. Furthermore, the isotropy relation $G = E/2(1+\nu)$ has been used. The simultaneous solution of equations (4)–(6) gives the relations among m, $\bar{P}$, $\bar{a}$ and $\bar{u}$ for given values of the surface roughness parameter α, the friction regime parameter β, the surface energy of adhesion parameter γ, the ratio (b/h), the Poisson's ratio (ν) and the height-dependent radius parameters (ε, ρ).

It is noted that due to adhesion during the unloading process, asperities may remain in contact even if the asperity overlap u is negative. This effect has been included by varying the adhesion radius ratio m to very large values in equations (4)–(6) when evaluating the force and contact area. However, when an asperity breaks free of its mating surface during unloading, its undeformed position may still maintain it within the distance h in which there is an attractive force of adhesion. The effect of these attractive forces on the applied normal force was neglected in [1], but is accounted for here.

Consider an elastic sphere in close proximity to an elastic half-space. If the minimum separation distance is greater than the adhesion distance h, then the interaction force vanishes. However, if the separation distance is less than h, a uniform tensile stress of magnitude σ_0 acts in a circular area of unknown radius c. The surface normal elastic displacement at the centre and along the periphery of the circle of interaction for such a loading are given in [29] by

$$u = \frac{2\sigma_0 c}{E^*}, \qquad u_C = \frac{4\sigma_0 c}{\pi E^*}, \tag{9}$$

respectively. At $r = c$, the separation after deformation must be equal to the adhesion separation (h) resulting in

$$\frac{c}{R'} = \left(\frac{4\sigma_0}{\pi E^*}\right) + \sqrt{\left(\frac{4\sigma_0}{\pi E^*}\right)^2 + 2\left(\frac{h-u}{R'}\right)}. \tag{10}$$

It is noted, however, that this solution is only valid if the elastic deformation at the centre of the circular area is insufficient to bring these bodies into contact. The normal force between the two bodies is given by $P = \pi c^2 \sigma_0$, which becomes

$$\bar{P} = -\frac{64\beta\gamma\lambda^3[g(\bar{z})]^2}{9(1-\nu)\alpha}\left[1 + \sqrt{1 + \frac{9\pi}{16\lambda^3 g(\bar{z})}\left(1 - \frac{u}{h}\right)}\right]^2. \tag{11}$$

An expression for the total non-dimensional normal force acting on the nominal contact area (including both contacting and noncontacting asperities) is obtained by integrating the normal force on individual asperities, resulting in the total normal force ($\bar{P}_T$):

$$\bar{P}_T = N\int_{\bar{d}-\bar{h}}^{\infty} \bar{P}\bar{\phi}(\bar{z})\,\mathrm{d}\bar{z} \tag{12}$$

where $\bar{h} = h/\sigma$. Thus, equation (12) has been modified to account for the forces exerted by noncontacting asperities by including equation (11) for values of $\bar{z}$ greater than $\bar{d} - \bar{h}$ but less than the value of $\bar{z}$ which causes the asperity to separate from the surface. For values of $\lambda > 0.655$, any asperity that separates will return to its undeformed position outside the Maugis range of adhesion. Thus, no correction for noncontacting asperities is needed for those cases.

2.2. Asperity friction model

Although adhesion affects the relationship between the normal force and the contact radius, it does not affect the relation between the frictional force and contact radius. From figure 2, the dimensionless shear stress is a function of the dimensionless contact radius and is approximated by

$$\ln\bar{\tau} = \begin{cases} \ln\bar{\tau}_1, & \bar{a} < \bar{a}_1, \\ M\ln\bar{a} + B, & \bar{a}_1 < \bar{a} < \bar{a}_2, \\ \ln\bar{\tau}_2, & \bar{a}_2 < \bar{a}, \end{cases} \tag{13}$$

where the left and right limits of region 2 are $(\bar{a}_1, \bar{\tau}_1)$ and $(\bar{a}_2, \bar{\tau}_2)$, respectively. The constants of equation (13) are given by

$$M = -\frac{\ln(\bar{\tau}_1/\bar{\tau}_2)}{\ln(\bar{a}_2/\bar{a}_1)}, \qquad B = \frac{\ln\bar{\tau}_1\ln\bar{a}_2 - \ln\bar{\tau}_2\ln\bar{a}_1}{\ln(\bar{a}_2/\bar{a}_1)}, \tag{14}$$

where M and B are, respectively, the slope and y-intercept of the line in region 2 of the log–log plot of figure 2. The frictional force F acting on a single asperity can be determined from equation (13) by using $F = \pi a^2\tau$ resulting in

$$\frac{F}{G^* b^2} = \begin{cases} \bar{\tau}_1\bar{a}^2, & \bar{a} < \bar{a}_1, \\ \mathrm{e}^B\bar{a}^{M+2}, & \bar{a}_1 < \bar{a} < \bar{a}_2, \\ \bar{\tau}_2\bar{a}^2, & \bar{a}_2 < \bar{a}. \end{cases} \tag{15}$$

The total dimensionless shear force $\bar{F}_T$ acting on the nominal contact area can be calculated by integrating the shear forces acting on each asperity against the probability density function, i.e.

$$\bar{F}_T = \frac{F_T}{Gb^2} = N\int_{\bar{d}-\bar{h}}^{\infty} \bar{F}\phi(\bar{z})\,\mathrm{d}\bar{z}, \qquad \bar{F} = \frac{F}{Gb^2} \tag{16}$$

in which the frictional force vanishes for noncontacting asperities. It is noted that for values of the applied tangential force F_T less than that given by equation (16), the distribution of tangential and normal forces among the asperities may cause some asperities to slip while others continue to stick. However, when F_T reaches the value given in equation (16) all contacting asperities will slide resulting in global slip. Thus, the coefficient of friction μ for two real surfaces separated by a distance $\bar{d}$, can be obtained from equations (1), (12) and (16).

2.3. Asperity height distributions

In [1], a Gaussian distribution of asperity heights was assumed, i.e.

$$\bar{\phi}(\bar{z}) = \frac{1}{(2\pi)^{1/2}} \exp\left(\frac{-\bar{z}^2}{2}\right). \tag{17}$$

In this paper, we investigate the effect of asymmetry by using a Weibull function, i.e.

$$\phi(\hat{z}) = \frac{\omega \hat{z}^{\omega-1}}{\eta^{\omega}} \mathrm{e}^{-(\hat{z}/\eta)^{\omega}}, \qquad \hat{z} > 0, \tag{18}$$

to represent the asperity height distribution. For this two-parameter Weibull function the mean (z_{M}), standard deviation of asperity heights (σ), skew (S) and kurtosis (K) are given in terms of the two Weibull parameters (ω,η) [30].

The Weibull distribution variable ($\hat{z}$) is then shifted by

$$z = \hat{z} - z_{\mathrm{M}}, \qquad z_{\mathrm{M}} = \eta B_1, \qquad B_n = \Gamma\left(1 + \frac{n}{\omega}\right), \tag{19}$$

where Γ is the gamma function, so that $z = 0$ corresponds to the mean of asperity heights. Furthermore, using the non-dimensional variable ($\bar{z} = z/\sigma$)

$$\bar{\phi}(\bar{z}) = \omega C^{\omega} \bar{z}^{\omega-1} \mathrm{e}^{-(C\bar{z})^{\omega}}, \qquad C = (B_2 - {B_1}^2)^{1/2} \tag{20}$$

is obtained. Note that this form of the Weibull distribution depends on only one parameter (ω) and that $\bar{z} = 0$ corresponds to the mean of asperity heights. The skew, standard deviation and kurtosis are given by

$$\begin{aligned} \bar{S} &= \frac{B_3 - 3B_2B_1 + 2B_1^3}{C^3}, \\ \sigma &= \eta C, \\ \bar{K} &= \frac{B_4 - 4B_3B_1 + 6B_2B_1^2 - 3B_1^4}{C^4}, \end{aligned} \tag{21}$$

respectively. It follows that these non-dimensional quantities also depend only on the parameter ω. As ω is varied, both the skew and kurtosis change. However, it is not possible to change the skew without also changing the kurtosis, as indicated by equation (21).

3. Results and discussion

In figure 3 we show the effect of noncontacting asperities on the friction coefficient. For a given applied force, the adhesive force on these asperities serves to increase the contact force and hence increase the contact area and frictional force, thereby giving a larger friction coefficient. As discussed previously, for $\lambda > 0.655$ the effect of noncontacting asperities vanishes. Figure 3 shows results with and without noncontacting asperities for $\alpha = 0.01$, $\gamma = 0.001$ and with $\beta = 1000$ ($\lambda = 0.523$) as well as with $\beta = 500$ ($\lambda = 0.415$). These cases represent the lowest values of λ used in [1]. The maximum effect on the friction coefficient is 2.1% for $\lambda = 0.523$ and 3.8% for $\lambda = 0.415$. As was explained above, this maximum difference corresponds to the smallest applied load.

Results have been obtained for the friction coefficient as a function of the normal load, for various values of the skew ($\bar{S}$) and the three key parameters (α, β, γ) defined in the AMM model. Figure 4 shows the effect of skew for the default values ($\alpha = 0.01, \beta = 1000, \gamma = 0.001$) used in [1]. Positive/negative skew is seen to decrease/increase both the friction coefficient as well as its variation with normal load. This result is due to negative skew causing more asperities to be above the mean of asperity heights than below. Correspondingly, there is less of a variation in height distribution for the $z > 0$ portion than for $z < 0$. The more lightly loaded the contact, the larger is the fraction of the Weibull distribution that is in contact. Thus, the asymmetry in the height distribution causes the surface to appear as if its roughness is reduced for lightly loaded contacts.

Figures 5–7 show similar results for a lower value of the surface roughness parameter ($\alpha = 0.006$), for a lower value of the friction regime parameter ($\beta = 500$) and for a higher value of the adhesion parameter ($\gamma = 0.002$), respectively. The smoother surface shows a greater effect of skew than the rougher one. This result may be expected based on the previous

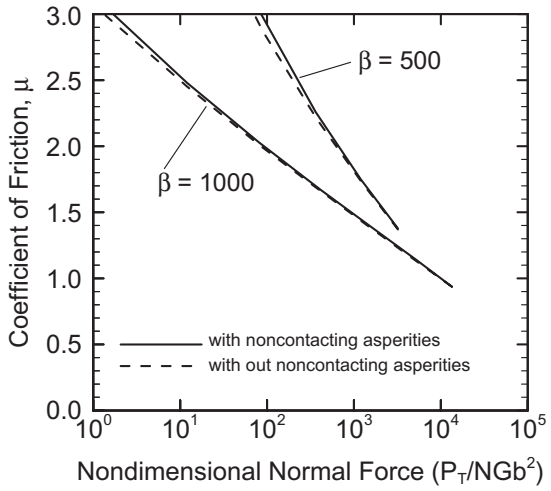

Figure 3. Effect of noncontacting asperities on the friction coefficient for $\alpha = 0.01$, $\gamma = 0.001$ and with $\beta = 1000$ ($\lambda = 0.523$) and $\beta = 500$ ($\lambda = 0.415$).

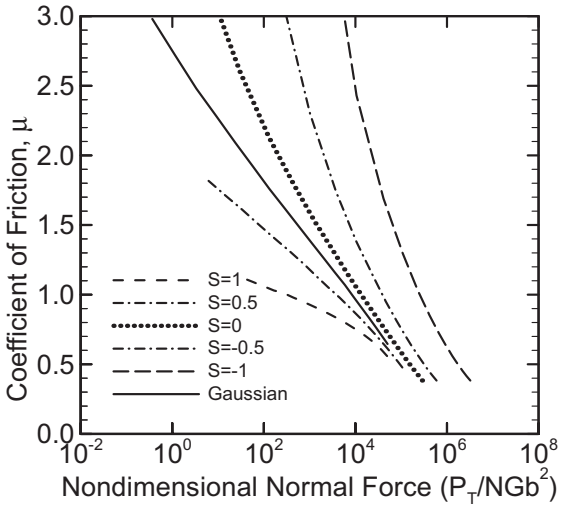

Figure 4. Coefficient of friction versus normal load for various skews and $\alpha = 0.01$, $\beta = 1000$, $\gamma = 0.001$.

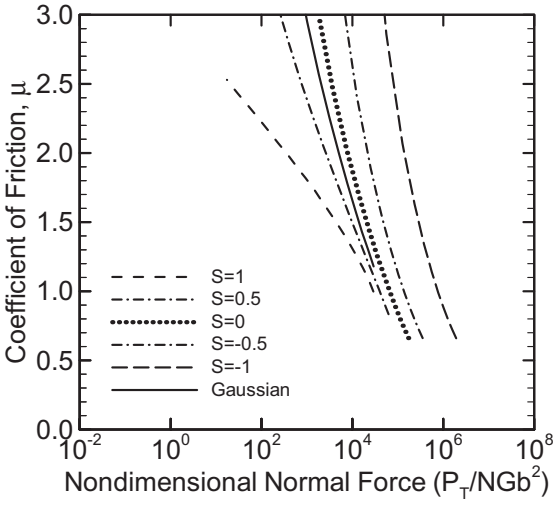

Figure 5. Coefficient of friction versus normal load for various skews and $\alpha = 0.006$, $\beta = 1000$, $\gamma = 0.001$.

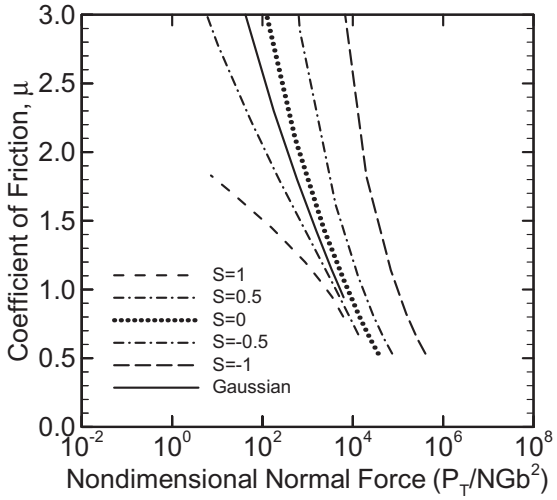

Figure 6. Coefficient of friction versus normal load for various skews and $\alpha = 0.01$, $\beta = 500$, $\gamma = 0.001$.

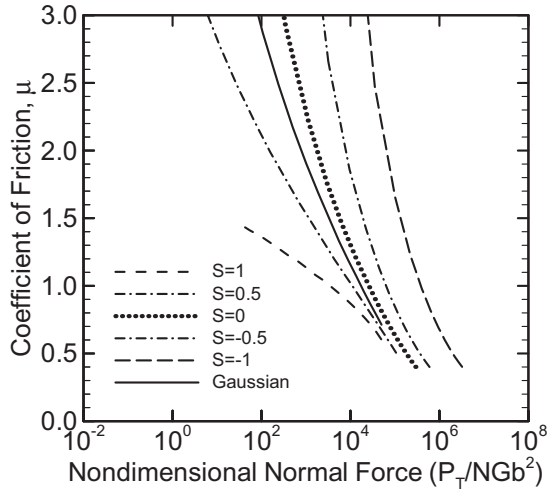

Figure 7. Coefficient of friction versus normal load for various skews and $\alpha = 0.01$, $\beta = 1000$, $\gamma = 0.002$.

Table 1. Values of the Weibull shape parameter (ω) and the corresponding dimensionless mean ($\bar{z}_M$), skew ($\bar{S}$), and kurtosis ($\bar{K}$).

Parameter (ω)	Mean ($\bar{z}_M$)	Skew ($\bar{S}$)	Kurtosis ($\bar{K}$)
40.74	32.32	−1	4.773
7.493	6.340	−0.5	3.258
3.602	3.243	0.0	2.716
2.216	2.098	0.5	3.028
1.564	1.530	1.0	4.159

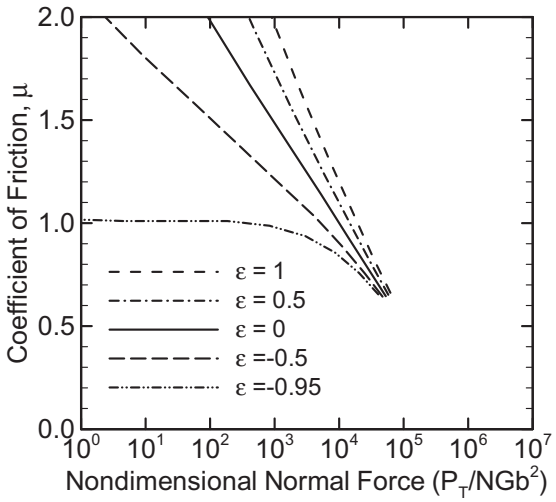

Figure 8. The variations of the friction coefficient with applied force, for various values of the parameter ε, with $\alpha = 10^{-2}$, $\beta = 10^3$, $\gamma = 10^{-3}$, $\rho = 1/2$.

discussion. The effect of a reduction of the friction regime parameter is to increase friction for the Gaussian distribution. However, as the skew decreases to the value of −1 the effect of β on friction decreases. The effect of an increase in the surface energy parameter is to increase friction for both positive and negative skew values.

It is noted that the friction results for the Gaussian distribution do not correspond exactly to the zero skew case of the Weibull distribution. This difference is because the Weibull distribution only approximates a Gaussian distribution. For lightly loaded contacts the difference between these two distributions in their 'leading edge' is sufficient to produce these discrepancies. The values of the Weibull shape parameter (ω), the mean ($\bar{z}_M$) the skew ($\bar{S}$) and kurtosis ($\bar{K}$) are shown in table 1.

Figures 8–10 show the variation of the friction coefficient with the applied force, each for five different values of the parameter ε $(1.0, 0.5, 0, -0.5, -0.95)$, all with $\rho = 0.5$, $\gamma = 10^{-3}$ and for different combinations of α and β. A positive/negative value of ε corresponds to taller asperities which have a greater/smaller radius of curvature than the shorter ones. For $\varepsilon = 1.0$, the tallest asperities have twice the radius as the average, whereas for $\varepsilon = -0.95$ the tallest asperities have a radius equal to 0.05 of the average. It is interesting to note that in all three cases shown (figures 8–10), an ε of −0.95 decreases friction and dramatically reduces the load-dependence of friction which was predicted in [1] for a

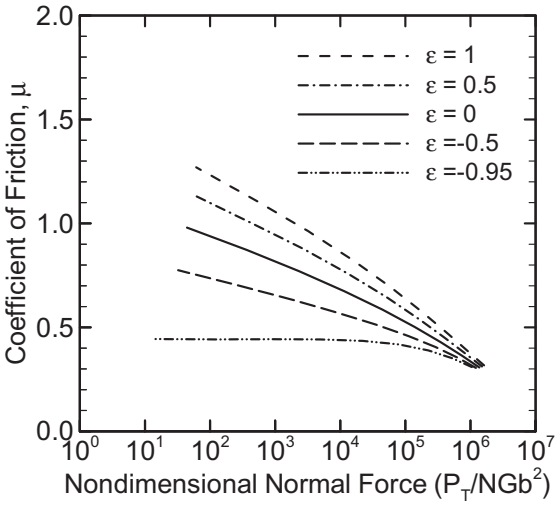

Figure 9. The variations of the friction coefficient with applied force, for various values of the parameter ε, with $\alpha = 10^{-2}$, $\beta = 5 \times 10^3$, $\gamma = 10^{-3}$, $\rho = 1/2$.

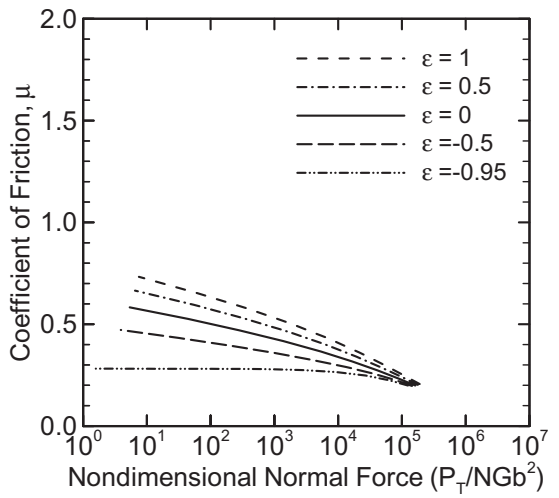

Figure 10. The variations of the friction coefficient with applied force, for various values of the parameter ε, with $\alpha = 3 \times 10^{-2}$, $\beta = 10^3$, $\gamma = 10^{-3}$, $\rho = 1/2$.

constant radius of curvature. Similarly, for $\varepsilon = 1.0$, friction is highest and so is its dependence on normal load. These results occur because for a given normal force, the contact area increases monotonically with the radius of curvature. Thus, a negative ε gives a smaller friction than positive ε. That trend is less pronounced for larger loads in which a greater portion of the asperities are in contact. The effect of height-dependent curvature is less for larger values of the friction regime parameter (figure 9) and for greater values of the surface roughness parameter (figure 10). The latter result can be explained because for a given load the contacting asperities will have a wider range of curvature for larger rather than smaller values of α, resulting in an averaging effect. The former effect is a consequence of the friction stress being less sensitive to radius in the micro-scale region (large β) than in the nano-scale regime (small β) of figure 2.

4. Conclusions

Three effects were included in a recently developed scale-dependent multi-asperity model of elastic contact and friction, which includes adhesion and scale-dependent friction. First, a Weibull distribution of asperity heights was used, which allows the skew and kurtosis to be varied, but not independently of each other. The results obtained demonstrate that positive/negative skew decreases/increases both the friction coefficient and its dependence on the normal load. Second, the effect of non-constant radii of curvature of the asperity summits, with the curvature varying with asperity height, was examined. This effect can be significant. For radii of curvature that increase/decrease with height, it was found that the friction coefficient increases/decreases as does its dependence on load. The effect of noncontacting asperities was found to be small because the original model [1] includes those asperities that are in contact only because of the attractive force of adhesion.

References

[1] Adams G G, Müftü S and Mohd Azhar N 2003 A scale-dependent model for multi-asperity model for contact and friction *ASME J. Tribol.* **125** 700–8
[2] Tabor D 1981 Friction—the present state of our understanding *ASME J. Lubrication Technol.* **103** 169–79
[3] Greenwood J A and Williamson J B P 1966 Contact of nominally flat surfaces *Proc. R. Soc. Lond.* A **295** 300–19
[4] Whitehouse D J and Archard J F 1970 The properties of random surfaces of significance in their contact *Proc. R. Soc. Lond.* A **316** 97–121
[5] Onions R A and Archard J F 1972 The contact of surfaces having a random structure *J. Phys. D: Appl. Phys.* **6** 289–304
[6] Johnson K L, Kendall K and Roberts A D 1971 Surface energy and the contact of elastic solids *Proc. R. Soc. Lond.* A **324** 301–13
[7] Derjaguin B V, Muller V M and Toporov Y P 1975 Effect of contact deformations on the adhesion of particles *J. Colloid Interface Sci.* **53** 314–26
[8] Tabor D 1977 Surface forces and surface interactions *J. Colloid Interface Sci.* **58** 2–13
[9] Maugis D 1992 Adhesion of spheres: the JKR-DMT transition using a Dugdale model *J. Colloid Interface Sci.* **150** 243–69
[10] Chang R W, Etsion I and Bogy D B 1987 An elastic-plastic model for the contact of rough surfaces *ASME J. Tribol.* **109** 257–63
[11] Chang R W, Etsion I and Bogy D B 1988 Adhesion model for metallic rough surfaces *ASME J. Tribol.* **110** 50–6
[12] Chang R W, Etsion I and Bogy D B 1988 Static friction coefficient model for metallic rough surfaces *ASME J. Tribol.* **110** 57–63
[13] Fuller K N G and Tabor D 1975 The effect of surface roughness on the adhesion of elastic solids *Proc. R. Soc. Lond.* A **345** 327–42
[14] Stanley H M, Etsion I and Bogy D B 1990 Adhesion of contacting rough surfaces in the presence of sub-boundary lubrication *ASME J. Tribol.* **112** 98–104
[15] Polycarpou A A and Etsion I 1998 Static friction of contacting real surfaces in the presence of sub-boundary lubrication *ASME J. Tribol.* **120** 296–303
[16] Kogut L and Etsion I 2003 A finite element based elastic-plastic model for the contact of rough surfaces *Tribol. Trans.* **46** 383–90
[17] Kogut L and Etsion I 2004 A static friction model for elastic-plastic contacting rough surfaces *ASME J. Tribol.* **126** 34–40

[18] Kotwal C A and Bhushan B 1996 Contact analysis of non-Gaussian surfaces for minimum static and kinetic friction and wear *Tribol. Trans.* **39** 890–8
[19] McCool J I 2000 Extending the capability of the Greenwood Williamson microcontact model *ASME J. Tribol.* **122** 496–502
[20] Yu N and Polycarpou A A 2002 Contact of rough surfaces with asymmetric distribution of asperity heights *ASME J. Tribol.* **124** 367–76
[21] Yu N, Pergande S R and Polycarpou A A 2004 Static friction model for rough surfaces with asymmetric distribution of asperity heights *ASME J. Tribol.* **126** 626–9
[22] Hurtado J A and Kim K-S 1999 Scale effects in friction of single asperity contacts: Part I. From concurrent slip to single-dislocation-assisted slip *Proc. R. Soc. Lond.* A **455** 3363–84
[23] Hurtado J A and Kim K-S 1999 Scale effects in friction in single asperity contacts: Part II. Multiple-dislocation-cooperated slip *Proc. R. Soc. Lond.* A **455** 3385–400
[24] Rabinowicz E and Kaymaram F 1991 On the mechanism of failure of particulate rigid disks *Tribol. Trans.* **34** 618–22
[25] Etsion I and Amit M 1993 The effect of small normal loads on the static friction coefficient for very smooth surfaces *J. Tribol.* **115** 406–10
[26] Levinson O, Etsion I and Halperin G 2003 An experimental investigation of elastic plastic contact and friction of a sphere on flat *Proc. 2003 STLE/ASME International Joint Tribology Conf. (Pointe Vedra Beach, Florida)* Paper 2003 TRIB-2598 on CD-ROM
[27] Adams G G and Müftü S 2003 Asymmetric asperity height distributions in a scale-dependent model for contact and friction *Proc. 2003 STLE/ASME International Joint Tribology Conf. (Pointe Vedra Beach, Florida)* Paper 2003 TRIB-258 on CD-ROM
[28] Adams G G and Müftü S 2004 Height-dependent asperity radii of curvatures in a contact and friction model *Proc. 2004 ASME/STLE International Joint Tribology Conf. (Long Beach, California)* Paper TRIB2004-64349 on CD-ROM
[29] Johnson K L 1985 *Contact Mechanics* (Cambridge: Cambridge University Press)
[30] Johnson N and Kotz S 1970 *Continuous Univariate Distributions-I* (New York: Wiley)